



New MKLP-2 inhibitors in the paprotrain series: Design, synthesis and biological evaluations



Christophe Labrière^{a,†}, Sandeep K. Talapatra^b, Sylviane Thoret^a, Cécile Bougeret^c, Frank Kozielski^b, Catherine Guillou^{a,*}

^a Centre de Recherche de Gif, Institut de Chimie des Substances Naturelles, CNRS, 1 Avenue de la Terrasse, 91198 Gif-sur-Yvette, France

^b School of Pharmacy, University College London, Department of Pharmaceutical and Biological Chemistry, 29-39 Brunswick Square, London WC1N 1AX, UK

^c Biokinesis S.A.S. 5, Rue de la Baume, 75008 Paris, France

ARTICLE INFO

Article history:

Received 22 October 2015

Revised 17 December 2015

Accepted 23 December 2015

Available online 24 December 2015

Keywords:

MKLP-2 inhibitor

Indole

Cancer

Mitotic kinesin

Paprotrain

ABSTRACT

Members of the kinesin superfamily are involved in key functions during intracellular transport and cell division. Their involvement in cell division makes certain kinesins potential targets for drug development in cancer chemotherapy. The two most advanced kinesin targets are Eg5 and CENP-E with inhibitors in clinical trials. Other mitotic kinesins are also being investigated for their potential as prospective drug targets. One recently identified novel potential cancer therapeutic target is the Mitotic kinesin-like protein 2 (MKLP-2), a member of the kinesin-6 family, which plays an essential role during cytokinesis. Previous studies have shown that inhibition of MKLP-2 leads to binucleated cells due to failure of cytokinesis. We have previously identified compound **1** (paprotrain) as the first selective inhibitor of MKLP-2. Herein we describe the synthesis and biological evaluation of new analogs of **1**. Our structure–activity relationship (SAR) study reveals the key chemical elements in the paprotrain family necessary for MKLP-2 inhibition. We have successfully identified one MKLP-2 inhibitor **9a** that is more potent than paprotrain. In addition, *in vitro* analysis of a panel of kinesins revealed that this compound is selective for MKLP-2 compared to other kinesins tested and also does not have an effect on microtubule dynamics. Upon testing in different cancer cell lines, we find that the more potent paprotrain analog is also more active than paprotrain in 10 different cancer cell lines. Increased selectivity and higher potency is therefore a step forward toward establishing MKLP-2 as a potential cancer drug target.

© 2015 Elsevier Ltd. All rights reserved.

1. Introduction

Mitosis is a highly regulated process that separates the replicated sister chromatids equally into the daughter cells. One class of potent anticancer agents (taxanes: paclitaxel, docetaxel) targets microtubule (MT) dynamics. The mode of action of these drugs causes mitotic arrest and eventually cell death in certain tumor cell lines.¹ Although successful, innate or acquired resistance to tubulin-targeting drugs and side effects limit the use of these agents. This has led to intense study of other proteins involved in cell division such as mitotic kinases (Plk1 & Auroras) and kinesins and their evaluation as potential targets for drug development in cancer chemotherapy. The development of molecules with inhibitory

activity against such targets leads to the arrest of cell proliferation in animal models.²

Molecular motors of the kinesin superfamily are involved in intracellular transport as well as in different discrete steps of mitosis and cytokinesis. At least 16 distinct kinesins have been shown to be involved at different stages of the mitosis and the expression of several molecular motors is restricted to proliferous tissues.³ The selective inhibition of some of these motor proteins inhibits cell proliferation, a characteristic feature of cancer cells and such inhibitors reduce some of the side effects (peripheral neuropathies) associated with the use of taxanes or *vinca* alkaloids.^{4,5} The two most exploited kinesin targets are Eg5 (Kif11, KSP; kinesin-5 family member) and CENP-E (Kif10; kinesin-7 family member) with inhibitory compounds currently being evaluated in phase I and II clinical trials.^{3,6,7} The most advanced inhibitor is ARRY-520 now in phase III clinical trials against relapsed and refractory multiple myeloma.

MKLP-2 (also known as Kif20A, RabK6, RBK6, Rab6KIFL, Rabkinesin6), a member of the kinesin-6 family, plays an essential role

* Corresponding author. Tel.: +33 (0)1 69 82 30 75; fax: +33 (0)1 69 07 72 47.

E-mail address: catherine.guillou@cnrs.fr (C. Guillou).

† Present address: Institutt for kjemi, Fakultet for Naturvitenskap og Teknologi, Postboks 6050 Langnes N-9037 Tromsø, Norway.

during cytokinesis^{8,9} and is overexpressed in various cancers such as pancreatic cancer,^{10–13} bladder cancer,¹⁴ breast cancer, small-cell lung cancer,¹⁵ hepatocarcinogenesis,¹⁶ melanoma¹⁷ and gastric cancer.¹⁸ MKLP-2 is involved in the proliferation and migration of pancreatic cancer cells.¹⁰

MKLP-2 is weakly detectable or absent in the normal spleen, lymph nodes, pancreas, lung, brain, liver, kidney and skeletal muscle.¹⁹ MKLP-2 is involved in the relocation of proteins Aurora B²⁰ and Chromosome Passenger Complex (CPC: complex of Aurora B, INCENP, survivin and borealin)²¹ to the spindle midzone. MKLP-2 possesses a conserved motor domain and has MT plus end directed motility.²² It binds to MTs and hydrolyses ATP to generate mechanical force to move along MTs.²³

MKLP-2 silencing with small interfering RNA molecules resulted in defects in cytokinesis with formation of binucleated or multinucleated cells.²⁴ Recently, the level of MKLP-2 and its mRNA expression were shown to be increased in paclitaxel resistant breast cancer and is associated with poor survival.²⁵ These observations make MKLP-2 an interesting therapeutic target for the development of cancer drugs, for tackling breast cancer taxane resistance and to study MKLP-2's functions on the cellular level.

We have previously identified compound **1** (named paprotrain) as the first known inhibitor of MKLP-2. Compound **1** does not inhibit others members of the kinesin superfamily involved in mitosis. Our previous work showed that **1** is a reversible inhibitor and is uncompetitive with respect to ATP as well as non-competitive with MTs.^{24,26}

To take the study further and rationalize a structure–activity relationship (SAR), we delimited the structure of **1** into five regions: the pyridine ring (A), the indole ring (B), the double bond bridge (C), the nitrile function (D) and the substituent of the double bond (E) (Fig. 1).

In our preliminary work, a small SAR analysis highlighted three determinant structural requirements: (i) the indole ring, (ii) the presence and the position of the nitrogen atom in the pyridine ring and (iii) the geometry of the double bond. None of the previously synthesized analogs were more active than compound **1**.^{24,26} However, replacement of the pyridine ring by different substituted phenyl analogs, chemical substitution of the indole scaffold and modification of the central bridge (length, unsaturation or substitution degrees) have not been explored. Pursuing our research project on MKLP-2 inhibitors in the indole series, we describe herein the synthesis and biological evaluations of new analogs of paprotrain **1**.

2. Results

2.1. Chemistry

2.1.1. Modulation of the pyridine ring (A)

In order to evaluate the importance of the pyridine ring on MKLP-2 inhibition, a series of analogs with substituted aromatic rings was prepared. The synthesis of aromatic analogs **4a–n** was achieved following the strategy summarized in Scheme 1. Knoevenagel condensation of indol-3-ylacetonitrile **2** with commercially available benzaldehydes **3a–n** afforded compounds **4a–n**, respectively.²⁷

In order to incorporate a protic group into the aromatic ring, the synthesis of the hydroxylated compound **6** was envisaged (Scheme 2). Reaction of **5**²⁸ with **2** under non-protic conditions was performed in the presence of NaH in a 1/1 DMSO/*tert*-butyl methyl ether mixture solution to afford the corresponding MEM-protected derivative. Subsequent deprotection of the alcohol function by aqueous hydrochloric acid yielded the corresponding alcohol **6**.

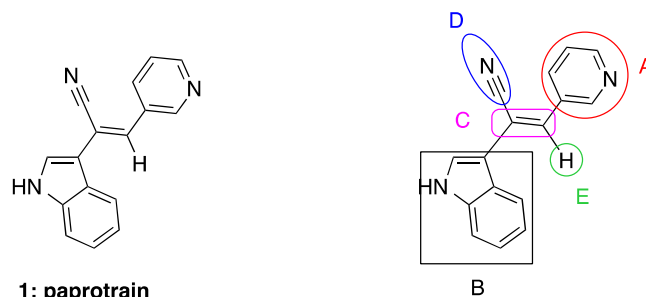
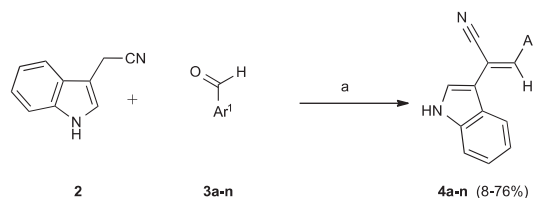


Figure 1. (a) Chemical structure of compound **1** (paprotrain). (b) Structure–activity relationship investigated by modifications carried out on the pyridine (A) and indole (B) rings, the double bond (C), the nitrile function (D) and the substituent of the double bond (E).



^a Reagents and conditions: Reactions are performed in darkness as follows: (a) MeONa, EtOH, RT or 40°C.

Scheme 1. Knoevenagel condensation allowing modulation of the A ring (see Table 1 for structures of compounds **4a–n**).

2.1.2. Modulation of the indole ring (B)

Preparation of analogs with a modified indole ring (compounds **9a–g**) was carried out by coupling the appropriate arylacetonitriles **7a–g** with the pyridine-3-carbaldehyde **8** (Scheme 3, Table 2). All arylacetonitriles were readily obtained following reported methodologies,^{29,30} except **7a–b**, which are commercially available.

The synthesis of analogs having an aromatic substituent in position 2 of the indole scaffold is depicted in Scheme 4. The 2-position of the indol-3-ylacetonitrile **2** was selectively brominated with *N*-bromosuccinimide to obtain compound **10**.³¹ The latter was then put in a reaction with phenyl boronic acid **11** or thiophen-3-yl boronic acid **12** under Suzuki conditions in the presence of PdCl₂(-PPh₃)₂ to give **13a** and **13b**, respectively. Knoevenagel condensation of aldehyde **8** with indolacetonitriles **13a–b** gave the expected indoles **14a–b**.

N-Methyl (i.e. **15a**) and *N*-acetyl (i.e. **15b**) analogs of **9a** were obtained in good yields by treating **9a** with methyl iodide and acetyl chloride, respectively (Scheme 5).

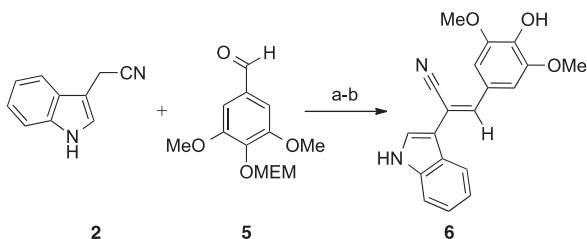
2.1.3. Modulation of the substituent of the double bond bridge (E)

A regio isomer of **1**, compound **18**, was prepared by treatment of pyridin-3-yl-acetonitrile **16** with 1*H*-indole-3-carbaldehyde **17** in the presence of sodium ethanolate formed in situ (Scheme 6).

2.1.4. Modulation of the double bond bridge (C)

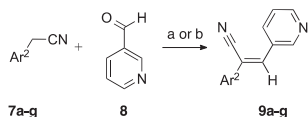
The reduced analog **19** was obtained by reduction of the central double bond of **1** with NaBH₄ (Scheme 7).

An analog (i.e. **22**) with a single one-atom linker between the indole and the pyridine skeleton was prepared following a two-step sequence. First, the 5-methoxyindole **20** was reacted with aldehyde **8**, to provide the alcohol **21** which was converted in situ to the corresponding tosylate. The nitrile **22** was then



^aReagents and conditions: (a) NaH, DMSO/MTBE, RT; (b) HCl aq., THF, RT (14% for 2 steps).

Scheme 2. Synthesis of compound **6**.



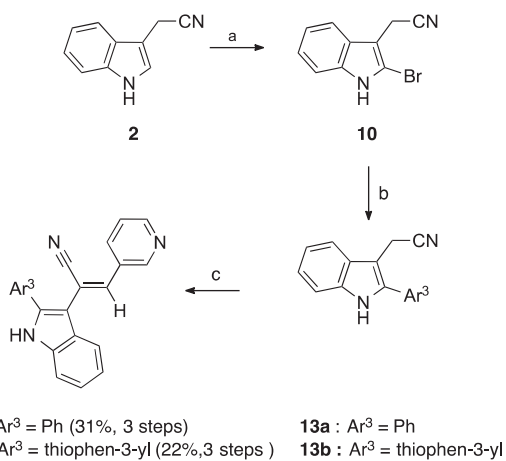
^aReagents and conditions: Reactions are performed in darkness as follows: (a) MeONa, MeOH or EtOH, 50°C for compounds **9a**, **9c–9g**; (b) NaH, DMSO/Et₂O, RT for compound **9b**.

Scheme 3. Syntheses of compounds **9** (see Table 2 for structures of compounds **9a–9g**).

obtained by substitution of the tosylate derivative with sodium cyanide (Scheme 8).

The synthesis of compound **25** with a three carbon central linker is shown in Scheme 9. Reaction of 5-methoxyindole **20** with anhydride derivatives of 2-cyanoacetic acid (produced in situ by brief heating of cyanoacetic acid **23** with acetic anhydride) in acetic anhydride furnished the β -ketonitrile **24**.³² Subsequent Knoevenagel condensation of **24** with pyridine-3-carbaldehyde **8** yielded **25** (Scheme 9).

Compound **29** with a central three-atom linker was synthesized to bring flexibility to the pyridine scaffold versus the indole and the nitrile. First, 5-methoxyindole **20** reacted with anhydride derivative of 2-(pyridin-3-yl)acetic acid hydrochloride **26** (produced in situ by reaction with acetic anhydride) to give the ketone **27**. Then, the indolic nitrogen of **27** was protected as a carbamate **28**. A Horner–Wadsworth–Emmons reaction between **28** and ethyl (cyanomethyl)phosphonate yielded the corresponding nitrile.



^aReagents and conditions: (a) NBS, silice, DCM, RT; (b) **11**: PhB(OH)₂ or **12**: thiophen-3-ylB(OH)₂, Na₂CO₃, PdCl₂(PPh₃)₂, Tol./ EtOH / H₂O, 80°C; (c) **8**, NaH, NMP, RT.

Scheme 4. Syntheses of compounds **14a–14b**.

Deprotection of the indole afforded the expected compound **29** (Scheme 10).

Knoevenagel condensation of the aldehyde **30**³³ with **7a** afforded the single isomer compound **31** bearing a four atoms linker (Scheme 11).

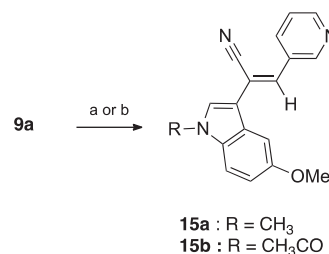
2.2. Biological results and discussion

To determine the effect of the newly synthesized analogs, we measured the inhibition of the basal and MT-stimulated MKLP-2 ATPase activities (Tables 1–3). Compound **1** (paprotrain) was used as a control. To investigate whether or not our analogs inhibit MT dynamics, their effects on tubulin polymerization and depolymerization were also evaluated. Paclitaxel, colchicine and docetaxel were used as control. Furthermore, their cytotoxicities were measured on KB human tumor cell lines. Finally, the selectivity for MKLP-2 was determined by measuring the inhibition of the MT-stimulated ATPase activity of several other kinesins.

2.2.1. Inhibition of MKLP-2

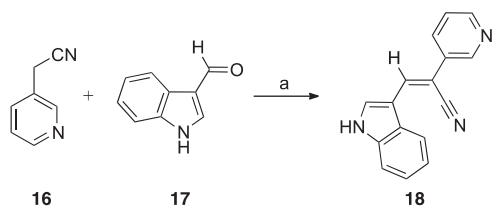
In the first series, the indole and the central double bond remain unchanged whereas different substituted phenyl rings replaced the pyridine ring of paprotrain **1**. Introduction of a methoxy group on the A ring (i.e. **4a**) or a chlorine atom (i.e. **4b**) in the same *meta* position as the nitrogen atom of the pyridine ring present in **1** results in a total loss of inhibition for MT stimulated MKLP-2 ATPase activity. Mono-functionalization of the phenyl ring in the *para* position with chlorine or fluorine results in decreased potency (i.e. **4d**, 25 fold and **4f**, 7 fold). Introduction of substituents in the *para* position as CF₃ (i.e. **4c**) or SMe (i.e. **4e**), disubstitution in positions *ortho–meta* (i.e. **4g**), *ortho–para* (i.e. **4h**) or *meta–para* (i.e. **4i**), trisubstitution (**4l–4n** and **6**) of the phenyl ring by methoxymethyl or hydroxy groups are also detrimental for the potency of the inhibitor analogs. Two disubstituted compounds (i.e. **4j** and **4k**) are less potent than **1** (3- and 11-fold, respectively) (Table 1).

In the second series, the unsubstituted indole ring of **1** was replaced by different indoles substituted in various positions.



^aReagents and conditions: (a) NaH, MeI, THF, RT for **15a** (99%); (b) MeCOCl, NEt₃, DMAP, THF/Pyr., RT for **15b** (90%).

Scheme 5. Syntheses of compounds **15a–15b**.

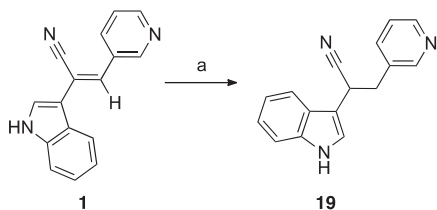


^aReagents and conditions: (a) Na, EtOH, RT (68%).

Scheme 6. Synthesis of compound **18**.

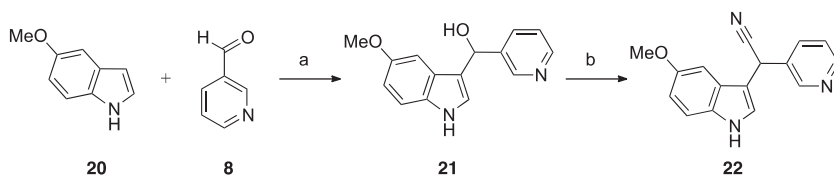
Introduction of a methoxy group in the 5-position of the indole (i.e. **9a**) increases the inhibition of basal and, especially, MT-stimulated ATPase activities (in comparison with compound **1**), whereas introduction of a larger substituent (a benzyloxy group, i.e. **9b**) leads to no inhibition of the basal activity and a decrease in the MT-stimulated ATPase activity. The presence of a methoxy group in the 6- or 4-position (i.e. **9c** and **9d** respectively) or introduction of a nitrogen atom in the 7-position of the indole (i.e. **9f**) decreases the inhibitory potency. A total loss of inhibition was observed when the 7-position (i.e. **9e**) is substituted by a methoxy. When large substituents such as phenyl (i.e. **14a**) or thiophene (i.e. **14b**) are present in the 2-position of the indole, a loss of inhibition was observed. N-alkylation (i.e. **15a**) or N-acylation (i.e. **15b**) of the indole ring lead to inactive compounds. Substitution of the 2-position by a smaller group, in this particular case by a methyl (i.e. **9g**), results in a loss of the basal ATPase activity. On the basis of results obtained in this second series, compound **9a** appears to be the most potent inhibitor of MKLP-2 ATPase activities (Table 2). The presence of a methoxy group in the 5-position of the indole ring probably leads to better interactions with the motor.

In the third series, modulations of the central linker were investigated. Compounds **1** and **9a** have a two carbon central linker. Shorter (one atom, i.e. **22**) or longer (three atoms, i.e. **25** or four atoms i.e. **31**) bridges between the indole and the pyridine rings lead to inactive molecules. The saturated analog of **1** (i.e. **19**) is



^aReagents and conditions: (a) NaBH₄, MeOH/THF, 60°C (40%).

Scheme 7. Synthesis of compound **19**.



^aReagents and conditions: (a) NaOH aq., MeOH, 0°C (75%); (b) 1-tosylimidazole, NaCN, NEt₃, TBAI, DMSO, 60°C (56%).

Scheme 8. Synthesis of compound **22**.

4-fold less active than **1**. Its vinylogous derivative **29** is inactive showing that the position of the nitrile function is also very sensitive. However, when the double bond is maintained, nitrile and vinylic hydrogen could be inverted to obtain compound **18** with activities quite similar to the ones observed for the saturated compound **19**. The presence of an acrylonitrile function (i.e. **1** and **9a**) appears to be a key element for the inhibition of MKLP-2 ATPase activities (Table 3).

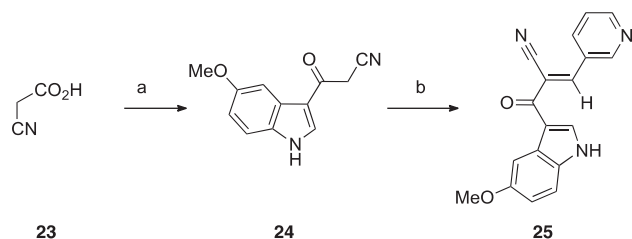
2.2.2. Influence on MT dynamics and cytotoxicity

In our previous work, in addition to binucleated cells, we also identified several other spindle defects when HeLa cells (human cervix carcinoma) were incubated with compound **1**, such as misaligned chromosomes and multipolar spindles.²⁴ These additional phenotypes could result from different roles of MKLP-2 at the later stages of mitosis where it assists in relocation of different proteins to the mid-body region that are essential for the completion of cell division. It is also worth mentioning that the phenotypes can also arise either from differences between the RNAi and small molecules techniques used, or could be due to targeting of other cellular proteins and not MKLP-2. We also observed that several of our analogs shown in Table 1 bear a (multi)methoxyphenyl scaffold, which is known to cause cytotoxicity by interfering with MT dynamics (inhibition of tubulin polymerization) such as with the molecules colchicine, podophyllotoxin or combretastatin.⁵ A prospective micromolar inhibitor of CENP-E (kinesin-7 family member) ATPase activity reported in the literature, UA62784, was later found to predominantly target MT dynamics by inhibiting tubulin polymerization.³⁴

We therefore decided to investigate whether our analogs influence MT dynamics and evaluated their effects in vitro by employing tubulin polymerization/depolymerization assays. In addition, their cytotoxicities were measured using the KB tumor cell line.

Several analogs of a first group of compounds (**4a**, **4c**, **4h–i**, **4l–m**, **6**, **14a–14b** and **15a**), which do not inhibit basal or MT-stimulated MKLP-2 ATPase activities, influence MT dynamics, and are weak to intermediate inhibitors of tubulin polymerization (IC₅₀ values between 9 and 115 μM). Their inhibition of tubulin polymerization activity in vitro is also reflected by their weak cytotoxic activity in cell-based assays on KB tumor cells. Whether this lack of activity is due to true poor cytotoxicity or a lack of transport of the compound into the cell has not been investigated and would require Caco-2 permeability assays. Majority of these compounds (**4c**, **4h–i**, **4l**, **14b**) inhibit tubulin polymerization, but not MT depolymerization. A few compounds (**4a**, **6**, **14a**, **15a**) inhibit both activities, a feature previously observed for other tubulin inhibitors.^{35,36}

Compounds of a second group (**4e**, **4g**, **4n**, **9e**, **15b**, **22**, **25**) do not inhibit MKLP-2 activity, have little or no effect on MTs dynamics, but still show a cytotoxic effect on KB cells at 10 μM inhibitor concentration, indicating that they must inhibit at least a third unknown cellular target.



^aReagents and conditions: (a) i) Ac_2O , 85°C ; (ii) **20**, Ac_2O , 110°C (95%); (b) **8**, MeONa , EtOH , RT (89%).

Scheme 9. Synthesis of compound **25**.

A third group of compounds (**4d**, **4f**, **4j–k**, **9c**, **9f**, **18**) inhibit MKLP-2 activity and influence MT dynamics and we hypothesize that their antiproliferative activity may result from at least, these two activities.

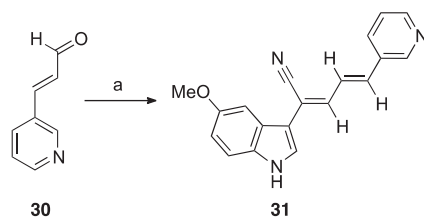
A last group of compounds (**1**, **4b**, **9a**, **9b**, **9d** and **9g**) inhibits MKLP-2 ATPase activities, but does not influence MT dynamics. These compounds display growth inhibition activity in KB cells, but whether or not they also interact with another protein target in addition to MKLP-2 cannot be concluded from the proliferation assays and will need more sophisticated cellular imaging techniques.

2.2.3. Further biological exploration of selected MKLP-2 inhibitors

The most interesting analog is compound **9a**, which is clearly more potent than **1** in inhibiting MKLP-2 ATPase activity, does not influence MT dynamics and exerts growth inhibition activity in KB tumor cells at $10\ \mu\text{M}$. Based on the results of the three complementary in vitro and cell-based assays, we conclude that there is a good window to develop more potent and specific MKLP-2 targeting analogs of paprotrain **1**.

We next tested the activity of the best inhibitors of MKLP-2, compounds **1** and **9a**, on a panel of ten human tumor cell lines listed in Table 4. Activities previously determined on KB are also indicated. Compound **9a** is more active than compound **1** on all cell lines with improvements ranging from ~2-fold for HCT116 (human colon carcinoma) to ~10-fold for MIA-PaCa-2 cells (human pancreatic carcinoma) with the exception of PK-59 (human pancreatic carcinoma) and HepG2 cells (human hepatocarcinoma), in which both compounds have no significant effect (Table 4). Both compounds show their highest anti-proliferative effects on K562 cells (human leukemia), in agreement with our previous study, in which we studied **1** in K562, HCT116, NCI-H1299, KB-3-1 and KB-V1 cells.²⁴

Compound **1** shows some influence on tubulin polymerization (Table 2). This behavior might contribute to the antiproliferative



^aReagents and conditions: (a) **7a**, MeONa , EtOH , 40°C (29%).

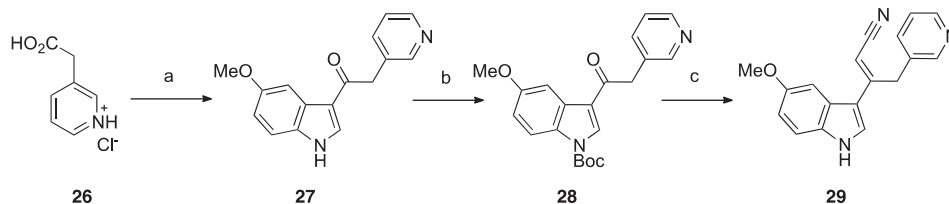
Scheme 11. Synthesis of compound **31**.

activities. On the other hand, **9a** did not influence both polymerization and depolymerization.

The specificity of compounds **9a–d** and **4k** for MKLP-2 was determined by measuring the inhibition of the MT-stimulated ATPase activity of seven kinesins (Table 5). Monastrol, a specific Eg5 inhibitor and AMP-PNP, a slowly hydrolysable ATP analog, were used as positive controls. These compounds do not inhibit the MT-stimulated ATPase activity of Centromere-associated protein E (CENP-E, kinesin-7 family), Kif4 (chromokinesin, kinesin-4 family), Eg5 (KSP, kinesin-5 family), conventional kinesin (Kif5b, kinesin heavy chain, kinesin-1 family), Kif3C (kinesin-3 family), Kifc3 (kinesin-14 family), nor Mitotic kinesin-like protein **1** (MKLP-1, kinesin-6 family) and are thus selective for MKLP-2. Interestingly, this family of inhibitors has no effect on the activity of MKLP-1, suggesting, they are highly selective within the kinesin-6 family members. These findings are in agreement with our previous publication, where we showed that **1** is specific for MKLP-2, tested on a panel of 11 human kinesins.²⁴

3. Conclusion

We have previously described paprotrain **1** as the first MKLP-2 inhibitor that induces apoptosis in a range of tumor cell lines.²⁴ In an effort to improve the efficiency of paprotrain, we have synthesized and evaluated novel series of paprotrain analogs. We show by in vitro and cell based assays that replacement of the pyridine ring by different substituted phenyl rings or modification of the central double bond lead to inactive or slightly less active compounds than paprotrain. However substitution of the indole ring by a methoxy group leads to compound **9a**, a new selective inhibitor of MKLP-2. **9a** is clearly more potent than paprotrain on the inhibition of MKLP-2 ATPase activities and it is 2- to 10-fold more potent in different human tumor cell lines. Very interestingly, its most significant potency gain (10-fold) was observed in MIA-PaCa-2 human pancreatic cancer cells. Taken together, the reported results indicate that analogs of paprotrain are promising compounds for the inhibition of human MKLP-2. Such compounds could be valuable tools to study MKLP-2 functions in cells and to treat MKLP-2 overexpressing tumors.



^aReagents and conditions: (a) i) Ac_2O , 85°C ; (ii) **20**, Ac_2O , 105°C (48%); (b) Boc_2O , DMAP , DCM , RT (93%); (c) (i) NaH , $(\text{EtO})_2\text{P}(\text{O})\text{CH}_2\text{CN}$, THF , RT; (ii) TFA , DCM , RT (71%).

Scheme 10. Synthesis of compound **29**.

4. Experimental section

4.1. Chemistry

4.1.1. General

All reactions were carried out under argon with dry solvents unless otherwise noted. Reactions were monitored by thin-layer chromatography on Merck silica gel plates (60F₂₅₄) with a fluorescent indicator. Yields refer to chromatographically or crystalline pure compounds. All commercially available reagents were used without further purification. All solvents were dried and distilled before use; CH₂Cl₂ was distilled from P₂O₅, THF was distilled from sodium/benzophenone, toluene on sodium, DMSO on magnesium sulfate, methanol and ethanol were distilled from Mg/I₂, pyridine and NEt₃ were distilled from KOH. All separations were carried out under flash chromatographic conditions on silica gel prepacked columns Redi Sep (230–400 mesh) at medium pressure (20 psi) by using a CombiFlash Companion. All new compounds gave satisfactory spectroscopic analyses (IR, ¹H NMR, ¹³C NMR, HRMS). NMR spectra were determined on a Bruker Avance-300 or on Bruker Avance-500. ¹H NMR spectra are reported in parts per million (δ) relative to the residual solvent peak. Data for ¹H are reported as follows: chemical shift (δ ppm), multiplicity (s = singlet, d = doublet, t = triplet, q = quartet, sxt = sextet, dd = double-doublet, m = multiplet), coupling constant in Hz, and integration. ¹³C NMR spectra were obtained using a Bruker Avance-300 (75.5 MHz) spectrometer and are reported in parts per million (δ) relative to the residual solvent peak. HRMS spectra were obtained on an E.S. I. TOF Thermoquest AQA Navigator spectrometer. Infrared (IR) (ν , cm⁻¹) spectra were recorded on a Fourier Perkin-Elmer Spectrum BX FT-IR. Melting points were measured in capillary tubes and are uncorrected. Elemental analyses were performed by the micro-analysis laboratory of the ICSN, CNRS, Gif-sur-Yvette. All the final compounds were purified to more than 95% purity. The purity of each compound was determined on an analytical reverse-phase Kinetex C18 2.6 μ m (4.6 \times 100 mm) via a Waters 2695 Alliance HPLC Separations Module coupled with a Waters W2996 Photodiode Array Detector at 390 nm; the detailed analytical conditions are available in the [Supplementary material section](#).

4.1.2. Synthesis

Specific procedures are described below. All the experimental procedures and detailed attribution of the different ¹H and ¹³C signals are available in the [Supplementary material section](#).

4.1.2.1. (Z)-2-(1H-Indol-3-yl)-3-(3-methoxy-phenyl)-acrylonitrile (4a). To a solution of sodium methanolate (260 mg, 4.80 mmol, 1.5 equiv) in anhydrous ethanol (15 mL) were added, under an argon atmosphere, (1H-indol-3-yl)-acetonitrile **2** (500 mg, 3.20 mmol, 1.0 equiv) and, after 30 min stirring, 3-methoxy-benzaldehyde **3a** (700 μ L, 5.76 mmol, 1.08 equiv). The reaction apparatus was protected from light and the mixture stirred at 40 °C for 11 h. The reaction was allowed to cool to room temperature and then, the solvent was removed under reduced pressure. The crude product was purified by silica gel flash-column chromatography (eluent: CH₂Cl₂, 100) to afford **4a** as a yellow powder (580 mg, 66%). TLC: R_f = 0.45 (CH₂Cl₂, 100). Mp 103 °C. IR ν_{\max} (cm⁻¹): 2219 (ν_{CN}), 3315 ($\nu_{\text{N-H}}$). ¹H NMR (d_6 -DMSO, 300 MHz) δ (ppm): 3.82 (3H, s), 6.99 (1H, dm, J = 7.8 Hz), 7.18 (1H, t, J = 7.8 Hz), 7.24 (1H, t, J = 7.8 Hz), 7.41 (1H, t, J = 7.8 Hz), 7.49 (2H, m), 7.51 (1H, s), 7.74 (1H, s), 7.79 (1H, s), 8.05 (1H, d, J = 7.8 Hz), 11.72 (1H, s). ¹³C NMR (d_6 -DMSO, 75.5 MHz) δ (ppm): 55.2, 102.0, 106.0, 110.6, 112.4, 113.7, 115.2, 118.4, 119.5, 120.5, 120.8, 122.5, 123.6, 126.7, 129.8, 135.9, 136.3, 137.2, 159.3; ESI-MS: m/z 297.1 ([M+Na]⁺). HRESI-MS: m/z 297.0997 (calcd for C₁₈H₁₄N₂O_{Na}, 297.1004). Anal. Calcd for C₁₈H₁₄N₂O, 0.2 H₂O:

C, 77.79; H, 5.22, N, 10.08; O, 6.91. Found: C, 77.77; H, 5.13; N, 10.23.

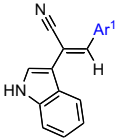
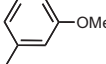
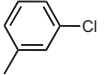
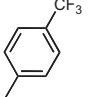
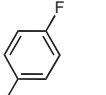
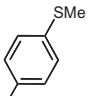
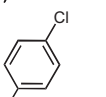
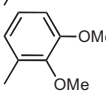
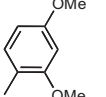
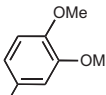
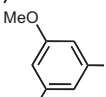
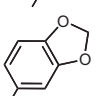
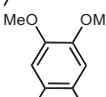
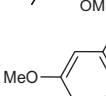
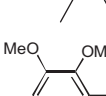
4.1.2.2. (Z)-3-(4-Hydroxy-3,5-dimethoxyphenyl)-2-(1H-indol-3-yl)-acrylonitrile (6). To a suspension of NaH (60 mg, 80%, 2.5 mmol, 1.7 equiv) in anhydrous DMSO (5 mL) was added, under an argon atmosphere, a solution of (1H-indol-3-yl)-acetonitrile **2** (277 mg, 1.8 mmol, 1.2 equiv) and 3,5-dimethoxy-4-(2-methoxyethoxymethoxy)-benzaldehyde **5** (400 mg, 1.5 mmol, 1.0 equiv) in a mixture of anhydrous DMSO (7 mL) and *tert*-butyl methyl ether (7 mL). The reaction apparatus was protected from light and the mixture was stirred at ambient temperature for 3 h, and then treated with brine (10 mL). The mixture was extracted with ethyl acetate (3 \times 30 mL), and the organic layer was washed with water and saturated aqueous ammonium chloride solution, dried over MgSO₄, filtered and concentrated in vacuo. To a solution of the resulting residue (130 mg) in THF (5 mL) was added a 2 M aqueous hydrochloric acid solution (4 mL). The reaction apparatus was protected from light and the mixture stirred at ambient temperature for 6 days. The mixture was poured into water, extracted with dichloromethane (3 \times 20 mL) and the organic layer was dried over MgSO₄. The solvent was removed under reduced pressure and then the residue was triturated with dichloromethane and *tert*-butyl methyl ether to afford **6** as a yellow powder (60 mg, 14% for two steps). TLC: R_f = 0.57 (CH₂Cl₂/MeOH, 96/4). Mp 245 °C. IR ν_{\max} (cm⁻¹): 2208 (ν_{CN}), 3329 ($\nu_{\text{N-H}}$). ¹H NMR (d_6 -DMSO, 500 MHz) δ (ppm): 3.84 (6H, s), 7.17 (1H, t, J = 7.8 Hz), 7.23 (1H, t, J = 7.8 Hz), 7.34 (2H, s), 7.48 (1H, d, J = 7.8 Hz), 7.65 (1H, s), 7.71 (1H, s), 8.07 (1H, d, J = 7.8 Hz), 9.03 (1H, s), 11.62 (1H, s). ¹³C NMR (d_6 -DMSO, 75.5 MHz) δ (ppm): 56.1, 102.1, 106.6, 111.0, 112.4, 119.3, 120.3, 122.4, 123.8, 124.9, 125.7, 137.2, 137.6, 147.9; ES-MS m/z 343.1 [M+Na]⁺. HRES-MS m/z 343.1044 (calcd for C₁₉H₁₆N₂O₃Na, 343.1059).

4.1.2.3. (Z)-2-(5-Methoxy-1H-indol-3-yl)-3-pyridin-3-yl-acrylonitrile (9a). To a solution of sodium ethanolate [prepared from sodium (350 mg, 15.2 mmol, 2.8 equiv) in anhydrous ethanol (30 mL)] were added, under an argon atmosphere, (5-methoxy-1H-indol-3-yl)-acetonitrile **7a** (1.0 g, 5.4 mmol, 1.0 equiv) and pyridine-3-carbaldehyde **8** (1 mL, 10.7 mmol, 2.0 equiv). The reaction apparatus was protected from light and the mixture was heated at reflux for 1 h. The reaction was allowed to cool to room temperature and then, the solvent was removed under reduced pressure. The mixture was extracted with ethyl acetate. The combined organic extracts were washed with brine and water, dried over MgSO₄, filtered and concentrated in vacuo. The crude product was purified by silica gel flash-column chromatography (eluent: CH₂Cl₂/MeOH, 98/2 to 97/3) and the residue triturated with ethanol and diethyl ether to afford **9a** as yellow crystals (1.08 g, 73%). TLC: R_f = 0.29 (CH₂Cl₂/MeOH, 97/3). Mp 175 °C. IR ν_{\max} (cm⁻¹): 2219 (ν_{CN}). ¹H NMR (d_6 -DMSO, 300 MHz) δ (ppm): 3.83 (3H, s), 6.90 (1H, dd, J = 8.9 Hz, J = 2.4 Hz), 7.40 (1H, d, J = 8.9 Hz), 7.48 (1H, d, J = 2.4 Hz), 7.52 (1H, dd, J = 8.1 Hz, J = 4.8 Hz), 7.74 (1H, s), 7.78 (1H, s), 8.32 (1H, d, J = 8.1 Hz), 8.58 (1H, dd, J = 4.8 Hz, J = 1.6 Hz), 8.98 (1H, d, J = 2.3 Hz), 11.65 (1H, s). ¹³C NMR (d_6 -DMSO, 75.5 MHz) δ (ppm): 55.6, 101.9, 108.2, 110.2, 112.4, 113.2, 118.1, 123.6, 124.0, 127.6, 130.9, 132.2, 134.6, 149.5, 149.9, 154.6; ES-MS m/z 276.1 [M+H]⁺, 298.1 [M+Na]⁺, 330.1 [M+Na+MeOH]⁺. HRES-MS m/z 276.110 (calcd for C₁₇H₁₄N₃O, 276.1137). Anal. Calcd for C₁₇H₁₄N₃O: C, 74.17; H, 4.76; N, 15.26, O, 5.81. Found: C, 73.89; H, 4.82; N, 15.33; O, 6.03.

4.1.2.4. (Z)-2-(5-Benzyloxy-1H-indol-3-yl)-3-pyridin-3-yl-acrylonitrile (9b). To a suspension of NaH (30 mg, 80%, 1.3 mmol, 1.6 equiv) in anhydrous DMSO (2.8 mL) was added, under an argon atmosphere, a solution of (5-benzyloxy-1H-indol-3-yl)-acetonitrile

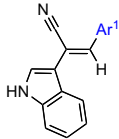
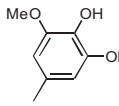
Table 1

Basal and MT-stimulated MKLP-2 ATPase inhibitory activities, influence on MT dynamics and growth inhibition activity in the KB human tumor cell line of novel paprotrain analogs (**1**, **4a–n** and **6**) in which the pyridine ring was replaced by substituted aromatic rings

Compound		Inhibition of MKLP-2 IC ₅₀ ^a (μM) (MIA (%))		Influence on MT dynamics (%) Poly./Depoly. ^b	Inhibition of KB tumor cell growth (%)	
		Basal	MT-stimulated		10 μM	1 μM
1 (paprotrain)		1.35 ± 0.2 (70%) ^a	0.83 ± 0.1 (95%)	11/n.i. ^c	27 ± 9	n.t. ^d
4a		n.i.	n.i.	37/38	89 ± 2	n.i.
4b		18.5 ± 2.4 (45%)	n.i.	n.i./n.i.	94 ± 2	19 ± 9
4c		n.i.	n.i.	57/n.i.	87 ± 9	n.i.
4d		34 ± 2.2 (84%)	29 ± 3.1 (73%)	22/n.i.	84 ± 6	n.i.
4e		n.i.	n.i.	n.i./n.i.	98 ± 3	n.i.
4f		10.1 ± 1.1 (40%)	8.9 ± 1.1 (34%)	13/n.i.	78 ± 16	n.t. ^d
4g		n.i.	n.i.	n.i./n.i.	100 ± 1	2 ± 1
4h		n.i.	n.i.	^e 76/n.i.	99 ± 2	35 ± 3
4i		n.i.	n.i.	^f 62/n.i.	99 ± 1	25 ± 4
4j		3.6 ± 1.5	10 ± 0.6	31/11	96 ± 1	31 ± 10
4k		14.3 ± 5.0 (70%)	5.1 ± 0.8 (82%)	35/n.i.	100 ± 1	11 ± 7
4l		n.i.	n.i.	32/n.i.	100 ± 2	40 ± 2
4m		n.i.	n.i.	n.i./13	83 ± 11	n.i.
4n		n.i.	n.i.	n.i./n.i.	81 ± 5	6 ± 11

(continued on next page)

Table 1 (continued)

Compound		Inhibition of MKLP-2 IC ₅₀ ^a (μM) (MIA (%))		Influence on MT dynamics (%) Poly./Depoly. ^b	Inhibition of KB tumor cell growth (%)	
		Basal	MT-stimulated		10 μM	1 μM
6		n.i.	n.i.	22/47	95 ± 1	59 ± 7
Paclitaxel	/	n.i.	n.i.	IC ₅₀ : 1.0 ± 0.1 μM/n.t.	n.t.	GI ₅₀ = 1 nM
Colchicine	/	n.i.	n.i.	IC ₅₀ : 2.0 ± 0.1 μM/n.t.	n.t.	GI ₅₀ = 4.2 nM
Docetaxel	/	n.i.	n.i.	n.t.	n.t.	GI ₅₀ = 0.13 nM

^a The numbers in parenthesis represent the maximal inhibition attained (MIA).

^b Poly.: polymerization, Depoly.: depolymerization.

^c n.i.: no inhibition.

^d n.t.: not tested.

^e IC₅₀: 12 ± 1 μM.

^f IC₅₀: 20 ± 5 μM.

7b (200 mg, 0.8 mmol, 1 equiv) and pyridin-3-carbaldehyde **8** (100 μL, 1.1 mmol, 1.4 equiv) in a mixture of anhydrous DMSO (4 mL) and diethyl ether (4 mL). The reaction apparatus was protected from light and the mixture was stirred at ambient temperature for 1h30, and then treated with brine. The mixture was extracted with ethyl acetate and the organic layer was washed with water and saturated aqueous ammonium chloride solution, and then dried over MgSO₄. The solvent was removed under reduced pressure, and the residue triturated with dichloromethane and diethyl ether to afford **9b** as a yellow powder (80 mg, 30%). TLC: R_f = 0.22 (heptane/EtOAc, 40/60). Mp 192 °C. IR ν_{max} (cm⁻¹) 2218 (ν_{CN}). ¹H NMR (d₆-DMSO, 300 MHz) δ (ppm): 5.19 (2H, s), 6.98 (1H, dd, J = 8.9 Hz, J = 2.3 Hz), 7.34 (1H, m), 7.39 (2H, m), 7.41 (1H, d, J = 8.9 Hz), 7.50 (2H, d, J = 7.2 Hz), 7.53 (1H, dd, J = 8.1 Hz, J = 4.8 Hz), 7.58 (1H, d, J = 2.3 Hz), 7.70 (1H, s), 7.78 (1H, s), 8.31 (1H, d, J = 8.1 Hz), 8.59 (1H, dd, J = 4.8 Hz, J = 1.5 Hz), 8.97 (1H, d, J = 2.1 Hz), 11.67 (1H, s). ¹³C NMR (d₆-DMSO, 75.5 MHz) δ (ppm): 70.0, 103.4, 108.2, 110.2, 113.1, 113.2, 118.0, 123.7, 123.9, 127.7, 127.8, 128.4, 130.9, 132.0, 132.4, 134.5, 137.6, 149.5, 149.9, 153.6; ES-MS m/z 352.1 [M+H]⁺, 374.1 [M+Na]⁺. HRES-MS m/z 352.1467 (calcd for C₂₃H₁₈N₃O, 352.1450).

4.1.2.5. (Z)-2-(2-Phenyl-1H-indol-3-yl)-3-(pyridin-3-yl)acrylonitrile (14a). To a solution of (1H-indol-3-yl)-acetonitrile **2** (700 mg, 4.5 mmol, 1.0 equiv) in CH₂Cl₂ (60 mL) were added silica (400 mg, 6.7 mmol, 1.5 equiv) and N-bromosuccinimide (800 mg, 4.5 mmol, 1.0 equiv) in portions. The reaction mixture was stirred at room temperature for 25 min and filtered. The filtrate was evaporated under vacuum. To a solution the resulting 2-bromoindole derivative **10** in toluene (40 mL) were added ethanol (20 mL), PhB(OH)₂ (1.1 g, 9.0 mmol), Na₂CO₃ (1.4 g, 13.4 mmol) and LiCl (570 mg, 13.4 mmol). The mixture was degassed before the addition of PdCl₂(PPh₃)₂ (380 mg, 0.54 mmol.). The reaction mixture was heated at 80 °C for 16 h. The reaction was allowed to cool to room temperature then water was added. The aqueous layer was extracted with EtOAc. The combined organic layers were washed with saturated aqueous Na₂CO₃ solution, dried over MgSO₄, filtered over silica and evaporated under vacuum. The resulting residue **13a** was dissolved in NMP (100 mL) and NaH (188 mg, 80%, 6.3 mmol) then pyridine-3-carbaldehyde **8** (760 μL, 8.1 mmol) were successively added. The mixture was stirred at room temperature for 2 h then quenched with saturated ammonium chloride aqueous solution and extracted with EtOAc. The combined organic layers were washed with water, brine, dried over MgSO₄ and evaporated under vacuo. The residue was purified

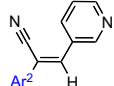
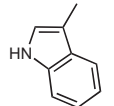
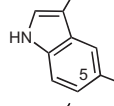
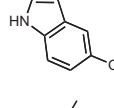
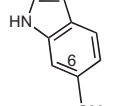
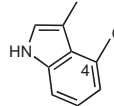
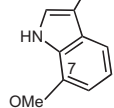
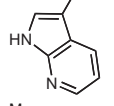
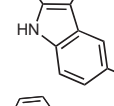
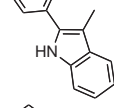
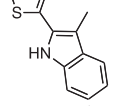
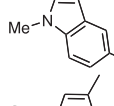
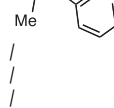
by silica gel flash-column chromatography (eluent: heptane/EtOAc, 50/50) to afford **14a** as a yellow powder (440 mg, 31%). IR ν_{max} (cm⁻¹): 2220 (ν_{CN}). ¹H NMR (d₆-DMSO, 500 MHz) δ (ppm): 7.18 (1H, t, J = 7.9 Hz), 7.25 (1H, t, J = 7.9 Hz), 7.45 (1H, m), 7.50 (1H, m), 7.53 (2H, m), 7.56 (1H, m), 7.62 (1H, s), 7.71 (2H, d, J = 7.6 Hz), 7.77 (1H, d, J = 7.9 Hz), 8.34 (1H, d, J = 7.9 Hz), 8.64 (1H, d, J = 4.9 Hz), 8.95 (1H, s), 11.96 (1H, s). ¹³C NMR (d₆-DMSO, 75.5 MHz) δ (ppm): 106.6, 111.9, 117.6, 118.4, 120.6, 122.7, 123.8, 126.6, 128.6, 128.7, 128.8, 130.2, 131.1, 134.7, 135.9, 137.1, 141.1, 150.0, 150.3; ESI-MS: m/z 322.1 ([M+H]⁺). HRES-MS: m/z 322.1352 (calcd for C₂₂H₁₆N₃⁺ 322.1344).

4.1.2.6. (Z)-2-(5-Methoxy-1-methyl-1H-indol-3-yl)-3-pyridin-3-yl-acrylonitrile (15a). To a solution of **9a** (200 mg, 0.7 mmol, 1.0 equiv) in THF (30 mL) was added NaH (44 mg, 60%, 1.1 mmol, 1.5 equiv) at 0 °C and, after 10 min stirring, methyl iodide (80 μL, 1.3 mmol, 1.8 equiv). The reaction apparatus was protected from light and the mixture stirred at room temperature for 3 h. Then saturated ammonium chloride aqueous solution was added and the mixture was extracted with EtOAc. The combined organic layers were washed with saturated aqueous Na₂CO₃ solution, dried (MgSO₄), filtered over celite and evaporated. The resulting residue was triturated with diethyl ether to afford **15a** as a yellow powder (210 mg, 99%). IR ν_{max} (cm⁻¹): 2216 (ν_{CN}). Mp 136 °C. ¹H NMR (d₆-DMSO, 500 MHz) δ (ppm): 3.82 (3H, s), 3.83 (3H, s), 6.96 (1H, dd, J = 8.9 Hz, J = 2.4 Hz), 7.46 (1H, d, J = 8.9 Hz), 7.49 (1H, d, J = 2.4 Hz), 7.52 (1H, dd, J = 8.1 Hz, J = 4.8 Hz), 7.71 (1H, s), 7.80 (1H, s), 8.30 (1H, d, J = 8.1 Hz), 8.57 (1H, dd, J = 4.8 Hz), 8.98 (1H, s). ¹³C NMR (d₆-DMSO, 75.5 MHz) δ (ppm): 32.9, 55.6, 102.2, 107.8, 109.1, 11.6, 112.3, 118.0, 123.6, 124.3, 130.8, 131.5, 131.8, 132.8, 134.5, 149.5, 149.9, 154.8; ESI-MS: m/z 290.2 ([M+H]⁺), 312.2 ([M+Na]⁺). HRES-MS: m/z 296.1286 (calcd for C₁₈H₁₆N₃O⁺ 296.1293). Anal. Calcd for C₁₈H₁₅N₃O, 0.2 H₂O: C, 73.80; H, 5.30; N, 15.34; O, 6.55. Found: C, 73.63; H, 5.44; N, 14.29.

4.1.2.7. (Z)-2-(1-Acetyl-5-methoxy-1H-indol-3-yl)-3-pyridin-3-yl-acrylonitrile (15b). To a solution of **9a** (200 mg, 0.7 mmol, 1.0 equiv) in THF (20 mL) and pyridine (5 mL) were added triethylamine (420 μL, 3.06 mmol, 4.2 equiv), acetyl chloride (220 μL, 3.06 mmol, 4.2 equiv) and DMAP (44 mg, 0.4 mmol, 0.5 equiv). The reaction apparatus was protected from light and the mixture stirred at room temperature for 48 h. Then saturated ammonium chloride aqueous solution was added and the mixture was extracted with EtOAc. The combined organic layers were washed with saturated aqueous Na₂CO₃ solution, dried (MgSO₄) and

Table 2

Basal and MT-stimulated MKLP-2 ATPase inhibitory activities, influence on MT dynamics and growth inhibition activity in the KB human tumor cell line of novel paprotrain analogs (**1**, **9a–g**, **14a–b** and **15a–b**) in which the unsubstituted indole was replaced by substituted indole

Compound		Inhibition of MKLP-2 IC ₅₀ (μM) (MIA (%)) ^a		Influence on MT dynamics (%) Poly./Depoly. ^b	Inhibition of KB tumor cell growth (%)	
		Basal	MT-stimulated		10 μM	1 μM
1 (Paprotrain)		1.35 ± 0.2 (70%) ^a	0.83 ± 0.1 (95%)	11/n.i. ^c	27 ± 9	n.t. ^d
9a		1.2 ± 0.1 (70%)	0.23 ± 0.02 (90%)	n.i./n.t.	57 ± 7	n.t.
9b		n.i. (40%)	1.3 ± 0.3 (70%)	12/n.i.	57 ± 4	n.t.
9c		5.6 ± 0.9 (85%)	5.4 ± 0.7 (90%)	54/n.i.	87 ± 2	78 ± 4
9d		4.2 ± 1.5 (80%)	3.3 ± 0.3 (90%)	n.i./n.i.	27 ± 8	n.t.
9e		n.i.	n.i.	n.i./n.i.	85 ± 3	n.i.
9f		11 ± 4.0 (40%)	10.2 ± 1.2 (75%)	19/n.i.	100 ± 1	29 ± 2
9g		n.i.	15.2 ± 1.8 (75%)	n.i./n.i.	69 ± 4	n.t.
14a		n.i.	n.i.	33/13	93 ± 1	n.i.
14b		n.i.	n.i.	^e 70/n.i.	99 ± 1	12 ± 2
15a		n.i.	n.i.	^f 53/15	33 ± 3	n.t.
15b		n.i.	n.i.	n.i./n.i.	74 ± 8	n.t.
Paclitaxel	/	n.i.	n.i.	IC ₅₀ : 1.0 ± 0.1 μM/n.t.	n.t.	GI ₅₀ = 1 nM
Colchicine	/	n.i.	n.i.	IC ₅₀ : 2.0 ± 0.1 μM/n.t.	n.t.	GI ₅₀ = 4.2 nM
Docetaxel	/	n.i.	n.i.	n.t.	n.t.	GI ₅₀ = 0.13 nM

^a The numbers in parenthesis represent the maximal inhibition attained (MIA).

^b Poly.: polymerization, Depoly.: depolymerization.

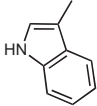
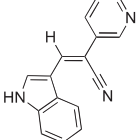
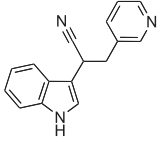
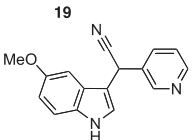
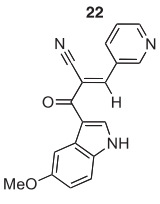
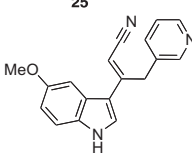
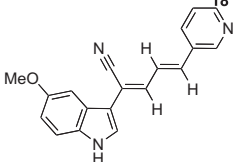
^c n.i.: no inhibition.

^d n.t.: not tested.

^e IC₅₀ = 9.2 ± 1 μM.

^f IC₅₀ = 115 ± 2 μM.

Table 3
Basal and MT-stimulated MKLP-2 ATPase inhibitory activities, influence on MT dynamics and growth inhibition activity in the KB human tumor cell line of novel paprotrain analogs (**18**, **19**, **22**, **25**, **29** and **31**) with modified central linker

Compound	Chemical Structure	Inhibition of MKLP-2 IC ₅₀ (μM) (MIA (%)) ^a		Influence on MT dynamics (%) Poly./Depoly. ^b	Inhibition of KB tumor cell growth (%)	
		Basal	MT-stimulated		10 μM	1 μM
1 (Paprotrain)		1.35 ± 0.2 (70%) ^a	0.83 ± 0.1 (95%)	11/n.i. ^c	27 ± 9	n.t. ^d
18		33.1 ± 3.8 (60%)	34.5 ± 9.5 (70%)	45/n.i.	23 ± 14	n.t.
19		59.0 ± 3.8 (35%)	29.8 ± 2.4 (72%)	16/21	5 ± 5	n.t.
22		n.i.	n.i.	n.i./n.i.	45 ± 3	n.t.
25		n.i.	n.i.	n.i./14	27 ± 10	n.t.
29		n.i.	n.i.	33/n.i.	n.i.	n.t.
31		n.i.	n.i.	11/n.i.	10 ± 6	n.t.
Paclitaxel		n.i.	n.i.	IC ₅₀ : 1.0 ± 0.1 μM/n.t.	n.t.	GI ₅₀ = 1 nM
Colchicine		n.i.	n.i.	IC ₅₀ : 2.0 ± 0.1 μM/n.t.	n.t.	GI ₅₀ = 4.2 nM
Docetaxel		n.i.	n.i.	n.t.	n.t.	GI ₅₀ = 0.13 nM

^a The numbers in parenthesis represent the maximal inhibition attained (MIA).

^b Poly.: polymerization, Depoly.: depolymerization.

^c n.i.: no inhibition.

^d n.t.: not tested.

evaporated. The residue was purified by silica gel flash-column chromatography (eluent: CH₂Cl₂/EtOH, 99/1 to 97/3) to afford **15b** as a beige powder (200 mg, 90%). IR ν_{max} (cm⁻¹): 2223 (ν_{CN}), 1694 ($\nu_{\text{C=O}}$). Mp 173 °C. ¹H NMR (*d*₆-DMSO, 500 MHz) δ (ppm): 2.72 (3H, s), 3.86 (3H, s), 7.09 (1H, dd, *J* = 8.9 Hz, *J* = 2.4 Hz), 7.52 (1H, d, *J* = 2.4 Hz), 7.60 (1H, dd, *J* = 7.9 Hz, *J* = 4.9 Hz), 8.03 (1H, s), 8.24 (1H, s), 8.34 (1H, d, *J* = 8.9 Hz), 8.39 (1H, d, *J* = 7.9 Hz), 8.67 (1H, dd, *J* = 4.9 Hz), 9.02 (1H, s). ¹³C NMR (*d*₆-DMSO, 75.5 MHz) δ (ppm): 24.1, 56.0, 103.4, 106.0, 114.3, 116.0, 117.3, 117.9, 124.3, 127.8, 128.1, 130.5, 130.7, 135.6, 139.6, 150.8, 151.1, 156.8, 169.8; ESI-MS: *m/z* 318.1 ([M+H]⁺), 340.1 ([M+Na]⁺). HRESI-MS: *m/z* 318.1235 (calcd for C₁₉H₁₆N₃O₂ 318.1243).

4.1.2.8. (Z)-3-(1H-Indol-3-yl)-2-pyridin-3-yl-acrylonitrile (**18**).

To a solution of sodium ethanolate [prepared from sodium (64 mg, 2.8 mmol, 1.6 equiv) in anhydrous ethanol (15 mL)] were added, under an argon atmosphere, pyridin-3-yl-acetonitrile **16** (235 μL, 2.2 mmol, 1.6 equiv) and, after 10 min stirring, 1H-indole-3-carbaldehyde **17** (200 mg, 1.4 mmol, 1.0 equiv). The reaction apparatus was protected from light and the mixture stirred at ambient temperature. Pyridine-3-acetonitrile (1.0 equiv) and sodium (1.5 equiv) were added after stirring for 21 h, and just sodium (1.5 equiv) after stirring for 47 h. The reaction was pursued for 89 h (136 h overall) at room temperature, the solvent removed under reduced pressure, and the crude purified by silica gel

Table 4
Evaluation of compounds **1** and **9a** against a panel of ten human tumor cell lines

Cell line	Tumor type	Compound 1 GI ₅₀ (μM)	Compound 9a GI ₅₀ (μM)
K562	Chronic myelocytic leukemia	21.6 ± 5.9	4.0 ± 0.3
A549	Non small cell lung carcinoma	>50	9.4
NCI-H460	Non small cell lung carcinoma	>50 (IC ₂₅ = 18.5)	8.2
MDA-MB-231	Mammary adenocarcinoma	>50	16.8
MCF7	Mammary adenocarcinoma	>50 (IC ₂₅ = 28.6)	15.8
HCT116	Colorectal carcinoma	>50	32.2
HT-29	Colorectal adenocarcinoma	>50 (IC ₂₅ = 7.5)	26.2
MIA-PaCa-2	Pancreatic carcinoma	>50	5.5
PK-59	Pancreatic carcinoma	>50	>50
HepG2	Hepatocarcinoma	>50	>50

flash-column chromatography (eluent: CH₂Cl₂/MeOH, 1/99 to 3/97). The residue was triturated with dichloromethane to afford **18** as a yellow powder (230 mg, 68%). TLC: *R*_f = 0.32 (CH₂Cl₂/MeOH, 98/2). Mp 89 °C. ¹H NMR (*d*₆-DMSO, 300 MHz) δ (ppm): 7.20 (1H, t, *J* = 7.2 Hz), 7.25 (1H, t, *J* = 7.2 Hz), 7.49 (1H, *J* = 8.1 Hz, *J* = 4.8 Hz), 7.53 (1H, d, *J* = 7.2 Hz), 8.11 (1H, d, *J* = 7.2 Hz), 8.16 (1H, d, *J* = 8.1 Hz), 8.37 (1H, s), 8.42 (1H, s), 8.54 (dd, *J* = 4.8 Hz, *J* = 1.4 Hz), 8.99 (d, *J* = 2.4 Hz), 12.06 (1H, s). ¹³C NMR (*d*₆-DMSO, 75.5 MHz) δ (ppm): 98.9, 110.8, 112.3, 118.9, 119.3, 120.8, 122.9, 123.8, 127.2, 127.7, 130.4, 132.2, 135.8, 136.2, 146.0, 148.5; ESI-MS 244.0 [M–H][−]. HRESI-MS: *m/z* 244.0880 (calcd for C₁₆H₁₀N₃, 244.0875). Anal. Calcd for C₁₆H₁₁N₃, 0.1 H₂O: C, 77.78; H, 4.57; N, 17.01. Found: C, 77.71; H, 4.73; N, 17.16.

4.1.2.9. 2-(1*H*-Indol-3-yl)-3-pyridin-3-yl-propionitrile (**19**).

To a solution of **1** (200 mg, 0.82 mmol, 1 equiv) in a mixture of THF (3 mL) and methanol (0.6 mL) was added, under an argon atmosphere, sodium borohydride (69 mg, 1.83 mmol, 3 equiv). The reaction mixture was stirred under microwave irradiation for 60 min at 115 °C and then, quenched with brine after cooling to room temperature. The mixture was extracted with ethyl acetate and the organic layer was washed with water and saturated aqueous ammonium chloride solution, and then dried over MgSO₄. The solvent was removed under reduced pressure, and the residue purified by silica gel flash-column chromatography

Table 5
Effect of compounds **9a–d** and **4k** on the MT-stimulated ATPase activity of seven human kinesins

Compound ^a	Inhibition MT-stimulated ATPase activity (−): no significant inhibition (<20% reduced activity compared to control) (+): significant inhibition (>30% reduced activity compared to control)						
	CENP-E	Kif4A	Eg5	Kif5b	Kif3C	Kif3	MKLP-1
9a	(−)	(−)	(−)	(−)	(−)	(−)	(−)
9b	(−)	(−)	(−)	(−)	(−)	(−)	(−)
9c	(−)	(−)	(−)	(−)	(−)	(−)	(−)
9d	(−)	(−)	(−)	(−)	(−)	(−)	(−)
4k	(−)	(−)	(−)	(−)	(−)	(−)	(−)
Monastrol ^b	(−)	(−)	(+)	(−)	(−)	(−)	(−)
AMP-PNP ^c	(+)	(+)	(+)	(+)	(+)	(+)	(+)

^a All compounds were tested in triplicate at a concentration of 15 μM except AMP-PNP, which was tested at 1 mM.

^b Monastrol, an Eg5 specific inhibitor, was included as a control.

^c AMP-PNP, a slowly-hydrolyzable ATP analog, was included as a general ATPase inhibitor.

(eluent: heptane/EtOAc, 60/40 to 20/80) to afford **19** as a beige powder (80 mg, 40%). TLC: *R*_f = 0.15 (heptane/EtOAc, 30/70). Mp 138 °C. IR *v*_{max} (cm^{−1}): 2239 (*v*_{CN}). ¹H NMR (*d*₆-DMSO, 500 MHz) δ (ppm): 3.32 (2H, m), 4.77 (1H, t, *J* = 7.3 Hz, H₂), 7.07 (1H, t, *J* = 7.9 Hz), 7.33 (2H, m), 7.41 (1H, d, *J* = 7.9 Hz), 7.70 (2H, d, *J* = 7.9 Hz, *J* = 7.9 Hz), 7.45 (2H), 11.17 (1H, s). ¹³C NMR (*d*₆-DMSO, 75.5 MHz) δ (ppm): 29.4, 35.7, 108.1, 111.9, 118.3, 119.1, 121.0, 121.7, 123.3, 123.8, 125.1, 133.1, 136.3, 136.7, 148.0, 150.2; ESI-MS: *m/z* 248.1 ([M+H]⁺). HRESI-MS: *m/z* 248.1195 (calcd for C₁₆H₁₄N₃, 248.1188).

4.1.2.10. (5-Methoxy-1*H*-indol-3-yl)-(pyridin-3-yl)-methanol (**21**).

To a solution 5-methoxyindole **20** (1 g, 6.8 mmol, 1.0 equiv) in methanol (8 mL) were added aqueous NaOH solution (80%, 200 μL, 4.0 mmol, 0.6 equiv) and pyridine-3-carbaldehyde **8** (800 μL, 8.5 mmol, 1.3 equiv). The reaction mixture was stirred at 0 °C for four hours then quenched with saturated aqueous ammonium chloride solution. The reaction mixture was extracted with EtOAc. The organic layer was washed with brine, dried (MgSO₄) and evaporated. The residue was purified by silica gel flash-column chromatography (eluent: CH₂Cl₂/EtOH, 96/4 to 94/6) to afford **21** as a rose powder (1.3 g, 75%). IR *v*_{max} (cm^{−1}): 3000–3400 (*v*_{O–H}). ¹H NMR (*d*₆-DMSO, 300 MHz) δ (ppm): 3.68 (3H, s), 5.73 (1H, d, *J* = 4.5 Hz), 5.99 (1H, d, *J* = 4.5 Hz), 6.70 (1H, dd, *J* = 8.7 Hz, *J* = 2.4 Hz), 6.95 (1H, d, *J* = 2.4 Hz), 7.06 (1H, s), 7.23 (1H, d, *J* = 8.7 Hz), 7.33 (1H, dd, *J* = 7.7 Hz, *J* = 4.7 Hz), 7.82 (1H, d, *J* = 7.7 Hz), 8.42 (1H, dd, *J* = 4.7 Hz, *J* = 1.7 Hz), 8.65 (1H, d, *J* = 1.9 Hz), 10.79 (1H, s). ¹³C NMR (*d*₆-DMSO, 75.5 MHz) δ (ppm): 55.8, 67.3, 101.8, 111.6, 112.6, 119.0, 123.6, 124.0, 126.3, 132.2, 134.3, 141.4, 148.2, 153.4; ESI-MS: *m/z* 255.1 ([M+H]⁺). HRESI-MS: *m/z* 255.1133 (calcd for C₁₅H₁₅N₂O₂, 255.1134).

4.1.2.11. 2-(5-Methoxy-1*H*-indol-3-yl)-2-(pyridin-3-yl)acetoneitrile (**22**).

To a solution of **21** (450 mg, 1.8 mmol, 1.0 equiv) in DMSO were added tosylimidazole (472 mg, 2.1 mmol, 1.2 equiv), triethylamine (614 μL, 4.4 mmol, 2.5 equiv), sodium cyanide (217 mg, 4.4 mmol, 2.5 equiv) and TBAI (66 mg, 0.2 mmol, 0.1 equiv). The reaction mixture was stirred at 60 °C for 2 h, and quenched with a saturated aqueous sodium carbonate solution. The mixture was extracted with ethyl acetate and the organic layer was washed successively with water, brine, and then dried over MgSO₄. The solvent was removed under reduced pressure, and the residue purified by silica gel flash-column chromatography (eluent: CH₂Cl₂/EtOH, 97/3) to afford **22** as a brown meringue (260 mg, 56%). TLC: *R*_f = 0.30 (CH₂Cl₂/EtOH, 96/4). IR *v*_{max} (cm^{−1}): 2244 (*v*_{CN}). ¹H RMN (*d*₆-DMSO, 300 MHz) δ (ppm): 3.70 (3H, s), 6.02 (1H, s), 6.79 (1H, dd, *J* = 8.9 Hz, *J* = 2.4 Hz), 6.94 (1H, d, *J* = 2.4 Hz), 7.31 (1H, d, *J* = 8.9 Hz), 7.35 (1H, s), 7.43 (1H, dd, *J* = 7.9 Hz, *J* = 4.9 Hz), 7.87 (1H, d, *J* = 7.9 Hz), 8.54 (1H, dd, *J* = 4.9 Hz, *J* = 1.6 Hz), 8.70 (1H, d, *J* = 2.4 Hz), 11.15 (1H, s, indolic H). ¹³C NMR (*d*₆-DMSO, 75.5 MHz) δ (ppm): 30.7, 55.3, 100.0, 108.4, 111.8, 112.8, 119.8, 124.0, 124.7, 125.1, 131.6, 135.0, 148.4, 149.0, 153.4; ESI-MS: *m/z* 264.1 ([M+H]⁺), 286.1 ([M+Na]⁺), 318.1 ([M+Na+MeOH]⁺). HRESI-MS: *m/z* 264.1133 (calcd for C₁₆H₁₄N₃O, 264.1137).

4.1.2.12. (E)-2-(5-Methoxy-1*H*-indol-3-carbonyl)-3-pyridin-3-yl-acrylonitrile (**25**).

To a suspension of sodium methanolate (139 mg, 2.6 mmol, 1.1 equiv) in anhydrous ethanol (50 mL) maintained at 0 °C were added, under an argon atmosphere, 5-methoxyindole **20** (500 mg, 2.3 mmol, 1.0 equiv) and, after 30 min stirring, pyridine-3-carbaldehyde **8** (263 μL, 2.8 mmol, 1.2 equiv). The reaction apparatus was protected from light and the mixture stirred at 0 °C for 2 h and then at room temperature for 38 h. The solvent was removed under reduced pressure and the residue purified by silica gel flash-column chromatography

(eluent: CH₂Cl₂/EtOH, 97/3). The product was triturated with dichloromethane and ethanol to afford **25** as a yellow powder (630 mg, 89%). TLC: *R*_f = 0.20 (CH₂Cl₂/EtOH, 96/4). Mp 225 °C. IR ν_{max} (cm⁻¹): 1579 ($\nu_{\text{C=O}}$), 2223 (ν_{CN}), 3188 ($\nu_{\text{N-H}}$). ¹H NMR (*d*₆-DMSO, 300 MHz) δ (ppm): 3.81 (3H, s), 6.93 (1H, dd, *J* = 8.8 Hz, *J* = 2.5 Hz, H6'), 7.46 (1H, d, *J* = 8.8 Hz), 7.64 (1H, dd, *J* = 8.1 Hz, *J* = 4.9 Hz), 7.71 (1H, d, *J* = 2.5 Hz), 8.27 (1H, s), 8.44 (1H, s), 8.32 (1H, d, *J* = 8.1 Hz), 8.74 (1H, dd, *J* = 4.9 Hz, *J* = 1.6 Hz), 9.08 (1H, d, *J* = 2.3 Hz), 12.24 (1H, s). ¹³C NMR (*d*₆-DMSO, 75.5 MHz) δ (ppm): 55.3, 103.2, 113.3, 113.4, 113.6, 117.2, 124.0, 126.9, 128.6, 131.5, 136.0, 136.5, 148.7, 151.4, 152.2, 155.9, 180.7; ESI-MS: *m/z* 304.1 ([M+H]⁺), 326.1 ([M+Na]⁺), 358.1 ([M+Na+MeOH]⁺), HRESI-MS: *m/z* 326.0916 (calcd for C₁₈H₁₃N₃O₂Na, 326.0905).

4.1.2.13. 1-(5-Methoxy-1*H*-indol-3-yl)-2-pyridin-3-yl-ethanone (27).

A mixture of 3-pyridylacetic (2.36 g, 13.6 mmol, 1.0 equiv) in acetic anhydride (12 mL) was heated in a sealed tube at 85 °C for one hour, then 5-methoxyindole (2 g, 13.6 mmol, 1.0 equiv) was added. The reaction mixture was heated at 85 °C for 20 min then at 105 °C for 30 min. After cooling to room temperature the mixture was quenched with water and EtOAc. The mixture was basified to pH 7 with saturated aqueous Na₂CO₃ solution. The mixture was extracted with EtOAc. The combined organic layers were washed with brine, dried (MgSO₄) and evaporated. The residue was purified by silica gel flash-column chromatography (eluent: CH₂Cl₂/EtOH, 96/4 to 94/6). The residue was triturated with ethanol and diethyl ether to afford **27** as a beige powder (1.74 g, 48%). IR ν_{max} (cm⁻¹): 3130 ($\nu_{\text{N-H}}$), 1621 ($\nu_{\text{C=O}}$). Mp 210 °C. ¹H NMR (*d*₆-DMSO, 500 MHz) δ (ppm): 3.75 (3H, s), 4.21 (2H, s), 6.85 (1H, dd, *J* = 8.7 Hz, *J* = 2.4 Hz), 7.34 (1H, dd, *J* = 7.9 Hz, *J* = 4.7 Hz), 7.38 (1H, d, *J* = 8.7 Hz), 7.67 (1H, d, *J* = 2.4 Hz), 7.73 (1H, d, *J* = 7.9 Hz), 8.44 (1H, dd, *J* = 4.7 Hz, *J* = 1.5 Hz), 8.51 (1H, s), 8.55 (1H, d, *J* = 1.5 Hz), 11.95 (1H, s). ¹³C NMR (*d*₆-DMSO, 75.5 MHz) δ (ppm): 42.4, 55.2, 102.9, 112.8, 115.7, 123.2, 126.3, 131.5, 132.1, 134.8, 137.0, 147.4, 150.4, 155.5, 191.7; ESI-MS: *m/z* 267.0 ([M+H]⁺). HRESI-MS: *m/z* 267.1132 (calcd for C₁₆H₁₅N₂O₂⁺ 267.1134). Anal. Calcd for C₁₆H₁₄N₂O₂, 0.2 H₂O: C, 71.20; H, 5.38; N, 10.38. Found: C, 71.08; H, 5.45; N, 10.31.

4.1.2.14. *tert*-Butyl 5-methoxy-3-[2-(pyridin-3-yl)acetyl]-1*H*-indol-1-carboxylate (28).

To a solution of **27** (1.00 g, 3.8 mmol, 1.0 equiv) and (Boc)₂O (1.2 mL, 5.6 mmol, 1.5 equiv) in CH₂Cl₂ was added DMAP (17 mg, 0.14 mmol, 0.04 equiv). The reaction mixture was stirred at room temperature for one hour. The solvent was removed under reduced pressure. The mixture was extracted with ethyl acetate. The combined organic extracts were washed with brine and water, dried over MgSO₄, filtered and concentrated in vacuo. The residue was purified by silica gel flash-column chromatography (eluent: EtOAc/EtOH, 100/0 to 90/10). The residue was triturated with diethyl ether to afford **28** as a white powder (1.28 g, 93%). IR ν_{max} (cm⁻¹): 1731 ($\nu_{\text{C=O}}$ carbamate), 1665 ($\nu_{\text{C=O}}$). ¹H NMR (*d*₆-DMSO, 500 MHz) δ (ppm): 1.69 (9H, s), 3.79 (3H, s), 4.42 (2H, s), 7.03 (1H, dd, *J* = 8.9 Hz, *J* = 2.1 Hz), 7.37 (1H, dd, *J* = 7.3 Hz, *J* = 4.7 Hz), 7.72 (1H, m), 7.73 (1H, d, *J* = 2.1 Hz), 7.99 (1H, d, *J* = 8.9 Hz), 8.47 (1H, d, *J* = 4.7 Hz), 8.53 (1H, s), 8.77 (1H, s). ¹³C NMR (*d*₆-DMSO, 75.5 MHz) δ (ppm): 28.1, 43.1, 55.8, 85.9, 104.5, 114.8, 116.1, 119.1, 123.8, 128.5, 129.9, 131.6, 134.6, 137.9, 148.2, 149.0, 151.2, 157.1, 193.8; ESI-MS: *m/z* 367.2 ([M+H]⁺), 389.1 ([M+Na]⁺), 755.3 ([2M+Na]⁺). HRESI-MS: *m/z* 367.1667 (calcd for C₂₁H₂₃N₂O₄⁺; *m/z* = 367.1658).

4.1.2.15. (*Z*)-3-(5-Methoxy-1*H*-indol-3-yl)-4-(pyridin-3-yl)-but-2-enitrile (29).

To a solution of diethyl(cyanomethyl)phosphonate (156 μ L, 1.5 mmol, 3.0 equiv) in THF (4 mL) was added NaH (44 mg, 80%, 1.5 mmol, 3.0 equiv). The reaction mixture was

stirred at room temperature for 30 min, then ketone **28** (180 mg, 0.5 mmol, 1.0 equiv) was added and the stirring was continued at room temperature for 12 h. The reaction was quenched with saturated ammonium chloride aqueous solution and extracted with EtOAc. The combined organic layers were washed with water, brine, dried over MgSO₄, filtered on silica and evaporated under vacuum to afford **14a** as a beige solid (100 mg, 71%). IR ν_{max} (cm⁻¹): 2201 (ν_{CN}). Mp °C. ¹H NMR (*d*₆-DMSO, 500 MHz) δ (ppm): 3.81 (3H, s), 4.22 (2H, s), 6.11 (1H, s), 6.84 (1H, dd, *J* = 8.9 Hz, *J* = 2.1 Hz), 7.30 (1H, dd, *J* = 7.6 Hz, *J* = 4.6 Hz), 7.32 (1H, m), 7.34 (1H, d, *J* = 8.9 Hz), 7.68 (1H, d, *J* = 7.6 Hz), 7.96 (1H, s), 8.39 (1H, d, *J* = 4.6 Hz), 8.60 (1H, s), 11.71 (1H, s). ¹³C NMR (*d*₆-DMSO, 75.5 MHz) δ (ppm): 37.2, 56.4, 90.8, 103.3, 113.4, 113.6, 114.0, 120.6, 124.5, 125.6, 131.1, 133.2, 135.3, 136.2, 148.6, 150.2, 155.9, 156.1; ESI-MS: *m/z* 290.1 ([M+H]⁺), 312.1 ([M+Na]⁺). HRESI-MS: *m/z* 312.1115 (calcd for C₁₈H₁₅N₃O₂Na⁺ 312.1113).

4.1.2.16. (2*Z*,4*E*)-2-(5-Methoxy-1*H*-indol-3-yl)-5-(pyridin-3-yl)penta-2,4-dienitrile (31).

To a solution of sodium methanolate (66 mg, 1.2 mmol, 1.2 equiv) in anhydrous ethanol (15 mL) were added, under an argon atmosphere, (5-methoxy-1*H*-indol-3-yl)acetonitrile **7a** (190 mg, 1.0 mmol, 1.0 equiv) and, after 30 min stirring, (*E*)-3-(pyridin-3-yl)acrylaldehyde **30** (150 mg, 1.1 mmol, 1.1 equiv). The reaction apparatus was protected from light and the mixture heated at 40 °C for 8 h. The reaction was allowed to cool to room temperature and then, the solvent was removed under reduced pressure and the crude taken up in ethyl acetate. The organic layer was washed with water and brine, dried over MgSO₄ and evaporated. The residue was purified by silica gel flash-column chromatography (eluent: CH₂Cl₂/EtOH, 99/1 to 98/2) to afford **31** as an orange powder (90 mg, 29%). TLC: *R*_f = 0.30 (CH₂Cl₂/EtOH, 96/4). Mp 223 °C. IR ν_{max} (cm⁻¹): 2212 (ν_{CN}). ¹H NMR (*d*₆-DMSO, 500 MHz) δ (ppm): 3.85 (3H, s), 6.90 (1H, dd, *J* = 8.9 Hz, *J* = 2.1 Hz), 7.26 (1H, d, *J* = 15.3 Hz), 7.37 (1H, dd, *J* = 15.3 Hz, *J* = 11.0 Hz), 7.40 (1H, d, *J* = 8.9 Hz), 7.44 (1H, dd, *J* = 7.9 Hz, *J* = 4.9 Hz), 7.47 (1H, d, *J* = 2.1 Hz), 7.64 (1H, d, *J* = 11.0 Hz), 7.75 (1H, s), 8.08 (1H, d, *J* = 7.9 Hz), 8.51 (1H, d, *J* = 4.9 Hz), 8.73 (1H, s), 11.67 (1H, s). ¹³C NMR (*d*₆-DMSO, 75.5 MHz) δ (ppm): 56.1, 102.6, 108.9, 110.2, 112.8, 113.7, 117.7, 124.5, 127.6, 128.0, 132.5, 132.8, 133.4, 134.2, 135.7, 149.2, 149.7, 155.1; ESI-MS: *m/z* 302.1 ([M+H]⁺), 324.1 ([M+Na]⁺). HRESI-MS: *m/z* 302.1296 (calcd for C₁₉H₁₆N₃O, 302.1293).

4.2. Biology

4.2.1. General

Competent BL21(DE3)pLysS cells were obtained from NOVAGEN. Chromatographic columns are from GE Healthcare. PIPES, ATP, lysozyme, DNase, EGTA, PMSF and kanamycin were obtained from Sigma-Aldrich. IPTG was purchased from Melford.

4.2.2. Measurements of the inhibition of basal and MT-stimulated MKLP-2 ATPase activities

MKLP-2₅₆₋₅₀₅ (N-terminal residues 56 to 505 of MKLP-2 covering the entire motor domain) was expressed and purified as previously described.¹⁶ Steady-state basal and MT-stimulated ATPase rates were measured using the pyruvate kinase/lactate dehydrogenase-enzyme linked assay.³⁰ The amounts of MKLP-2₅₆₋₅₀₅ were optimized at 4 μ M for basal and 40 nM for MT-stimulated activity assays. Assays were performed in the presence of increasing inhibitor concentrations (0 μ M to 100 μ M). All compounds were measured at least in triplicate. Paprotrain served as a positive control. Kinetics measurements were performed using a 96-well Sunrise photometer (TECAN, Maennedorf, Switzerland). The data were analyzed using Kaleidagraph 4.0 (Synergy Software).

4.2.3. Inhibition of tubulin polymerization

Sheep brain MTs were purified by two cycles of assembly/disassembly at 37 °C/0 °C in (2-[*N*-morpholino]ethanesulfonic acid, pH 6.6) (MES) buffer: 100 mM MES, 1 mM EGTA (ethyleneglycolbis [β -aminoethyl ether]-*N,N,N,N'*-tetraacetic acid), 0.5 mM MgCl₂. All samples were dissolved in DMSO. The evaluated compound (1 μ L) was added to a microtubules solution (150 μ L) that was incubated at 37 °C for 10 min and at 0 °C for 5 min. The tubulin polymerization rate was measured by turbidimetry at 350 nm according to Zavala and Guénard's protocol using deoxydopodophyllotoxin as a reference compound. For this assay, only differences >10% were considered significant.

4.2.4. Inhibition of tubulin assembly and disassembly

Sheep brain tubulin was purified by two cycles of assembly/disassembly and then dissolved in the assembly buffer containing 0.1 M MES, 0.5 mM MgCl₂, 1 mM EGTA and 1 mM GTP, pH 6.6 (the concentration of tubulin was about 2–3 mg/mL). Tubulin assembly was monitored and recorded continuously by turbidimetry at 350 nm in a UV spectrophotometer equipped with a thermostated cell at 37 °C, as previously described.^{35,36} The IC₅₀ value of each compound was determined as the concentration, which decreased the maximum assembly rate of tubulin by 50% compared to the rate in the absence of compound. The IC₅₀ values for all compounds were compared to the IC₅₀ of colchicine, measured the same day under the same conditions. For polymerization the compound analog was added to tubulin at 0 °C, the mixture was placed into a thermostated tank at 37 °C and the polymerization curve was observed during a few min. For MT depolymerization, tubulin was polymerized at 37 °C thermostat enabled tank for 10 min, the compound analog was added to MTs at 0 °C, and the depolymerization curve was observed during for next few minutes.

4.2.5. Inhibition of KB cell growth

KB (human epidermoid carcinoma) cells were grown in Dulbecco's modified Eagle's medium supplemented with 25 mM glucose, 10% (v/v) fetal calf serum, 100 UI penicillin, 100 μ g/ml streptomycin and 1.5 μ g/ml fungizone and kept under 5% CO₂ at 37 °C. 96-Well plates were seeded with 500 KB cells per well in 200 μ L medium. Twenty-four hours later, inhibitor analogs dissolved in DMSO were added for 72 h at a final concentration of 10⁻⁵ M (10 μ M) and 10⁻⁶ M (1 μ M) in a fixed volume of DMSO (1% final concentration). Controls received an equal volume of DMSO. Experiments were carried out in duplicate. The number of viable cells was measured at 490 nm with the MTS reagent (Promega, Madison, WI) and GI₅₀ values were calculated as the concentration of compound eliciting a 50% inhibition of cell proliferation.

4.2.6. Inhibition of K562, A549, NCI-H460, MDA-MB-231, MCF-7, HCT-116, HT-29, MIA-PaCa-2, PK59 and HepG2 cell growth

K562 (human chronic myelocytic leukemia), A549 and NCI-H460 (human lung carcinoma), MDA-MB-231 and MCF-7 (human breast carcinoma), HCT-116 and HT-29 (human colon carcinoma) MIA-PaCa-2 and PK-59 (human pancreatic carcinoma) and HepG2 (human hepatocarcinoma) cells were bought from ATCC or ECACC. K562 cells were grown in RPMI 1640 medium supplemented with 10% Fetal Bovine Serum (FBS) and 2 mM ultraglutamine, A549 cells were grown in RPMI 1640 medium supplemented with 10% FBS and 2 mM sodium pyruvate, NCI-H460 cells were grown in RPMI 1640 medium supplemented with 10% FBS, 10 mM HEPES, 1 mM Sodium pyruvate and 2.5 g/l glucose, MDA-MB-231 cells were grown in Ham's F12 medium supplemented with 10% FBS, MCF-7 cells were grown in EMEM medium supplemented with 10% FBS, 2 mM Ultraglutamine, 1 mM sodium pyruvate, 0.1 mM non-essential amino acids and 10 nM β -estradiol. HCT-116 and HT-29 cells

were grown in Mc Coy's 5A medium supplemented with 10% FBS and 0.5 mM Ultraglutamine. MIA-PaCa-2 cells were grown in DMEM medium supplemented with 10% FBS, PK-59 cells were grown in RPMI 1640 medium supplemented with 10% FBS, HepG2 cells were grown in EMEM medium supplement with 10% decompensated FBS, 0.1 mM non essential amino acids, 2 mM ultraglutamine and penicillin/streptomycin. Cells were kept under 5% CO₂ at 37 °C. On D0 (day 0), the cells were plated in 90 μ L in 96 wells plates at densities ranging from 500 to 5000 cells per well. On D1, the cells were treated with compounds at ten testing concentrations ranging from 0.0025 to 50 μ M final concentration in triplicates. On D4, the cell proliferation reagent WST-1 was added according to the standard operating procedures. The cells were then incubated for 30 min to 4 h at 37 °C and 5% CO₂. After these incubations, the absorbance was measured at 450 nm. The analysis of the results was performed with the Ascent software 2.6 (ThermoLabsystems, France), Microsoft Excel 2003 and GraphPad Prism 4.03 softwares to give the concentration of the compounds that induces the death of 50% of the cells (GI₅₀).

4.2.7. Inhibitory activity of compounds against the MT-stimulated ATPase activity of CENP-E, Kif4A, Eg5, Kif5B, KIF3C, KIF3, MCAK and MKLP-1 motor domains

CENP-E (Cytoskeleton, Cat. # CP01), Chromokinesin/Kif4A (Cytoskeleton, Cat. # CR01), Eg5 (Cytoskeleton, Cat. # EG01), Kif5B (Cytoskeleton, Cat. # KR01), KIF3C (Cytoskeleton, Cat. # KC01), KIF3C (Cytoskeleton, Cat. # KF01) and MKLP-1 (Cytoskeleton, Cat. # MP01) motor domains, expressed as GST fusion proteins as well as porcine brain MT (Cytoskeleton, Cat. # MT002) were used for specificity experiments. Monastrol was included as a control (Eg5 inhibitor) and AMP-PNP was included as a general ATPase inhibitor (inhibits kinesins). All experiments were performed in triplicate at 22 °C. Compounds were mixed in 7.5 mM PIPES-NaOH pH 7.0 buffer containing 5 μ M MgCl₂, 10 μ M Taxol, ELIPA 1 reagent (Cytoskeleton, Cat # BK051), ELIPA 2 reagent (Cytoskeleton, Cat # BK051) and 1.25 mg/mL MTs. Each motor domain was added to the mix at 15 μ M final concentration and the reaction was initiated by adding 1 mM Mg²⁺ATP. The reactions were measured in a SpectraMax M2 (Molecular Devices) set in kinetic mode at a wavelength of 360 nm.

Acknowledgements

We thank the CNRS, ICSN, Cancer Research UK (CR-UK) and Biokinesis for financial support. The PhD student C. Labrière was supported by a fellowship from the Institute de Chimie des Substances Naturelles (ICSN-CNRS). Some of the initial biochemical work forms part of the PhD thesis of S. Talapatra, the Beatson Institute for Cancer Research. We thank Prof. J. Y. Lallemand, Dr. C. Thal, Prof J.Y. Husson and Dr. F. Gueritte for their interest in our work. We are grateful to Drs. G. Aubert and T. Cresteil for performing the proliferation assays on KB cells. We also thank C-Ris Pharma, which performed the proliferation assays on the panel of human tumor cell lines, Cytoskeleton, which performed the inhibition assays on the panel of human kinesins and Leads to Development, which is specialized in non-clinical and early clinical development of therapeutic agents, for fruitful discussions.

Supplementary data

Supplementary data (all the experimental procedures and detailed attribution of the different ¹H and ¹³C signals. HPLC data of the final compounds) associated with this article can be found, in the online version, at <http://dx.doi.org/10.1016/j.bmc.2015.12.042>.

References and notes

1. Wood, K. W.; Cornwell, W. D.; Jackson, J. R. *Curr. Opin. Pharmacol.* **2001**, *1*, 370.
2. Huszar, D.; Theoclitou, M. E.; Skolnik, J.; Herbst, R. *Cancer Metastasis Rev.* **2009**, *28*, 197.
3. Rath, O.; Kozielski, F. *Nat. Rev. Cancer* **2012**, *12*, 527.
4. Orr, G. A.; Verdier-Pinard, P.; Mc Daid, H.; Horwitz, S. B. *Oncogene* **2003**, *22*, 7280.
5. Jordan, M. A.; Wilson, L. *Nat. Rev. Cancer* **2004**, *4*, 253.
6. El-Nassan, H. B. *Eur. J. Med. Chem.* **2013**, *62*, 614.
7. Liu, X.; Gong, H.; Huang, K. *Cancer Sci.* **2013**, *104*, 651.
8. Fontijn, R. D.; Goud, B.; Echard, A.; Jollivet, F.; van Marle, J.; Pannekoek, H.; Horrevoets, A. J. *Mol. Cell Biol.* **2001**, *21*, 2944.
9. Hill, E.; Clarke, M.; Barr, F. A. *EMBO J.* **2000**, *19*, 5711.
10. Stangel, D.; Erkan, M.; Bucholz, M.; Gress, T.; Michalski, C.; Raulefs, S.; Friess, H.; Kleef, J. *J. Surg. R.* **2015**, *197*, 91.
11. Taniuchi, K.; Furihata, M.; Saibara, T. *Neoplasia* **2014**, *1082*, 16.
12. Hidalgo, M.; Von Hoff, D. D. *Clin. Cancer Res.* **2012**, *18*, 4249.
13. Imai, K.; Hirata, S.; Irie, A.; Senju, S.; Ikuta, Y.; Yokomine, K.; Harao, M.; Inoue, M.; Tomita, Y.; Tsunoda, T.; Nakagawa, H.; Nakamura, Y.; Baba, H.; Nishimura, Y. *Br. J. Cancer* **2011**, *104*, 300.
14. Ho, J. R.; Chapeaublan, E.; Kirkwood, L.; Nicolle, R.; Benhamou, S.; Leuret, T.; Allory, Y.; Southgate, J.; Radvanyi, F.; Goud, B. *PLoS ONE* **2012**, *7*, e39469.
15. Kikuchi, T.; Daigo, Y.; Katagiri, T.; Tsunoda, T.; Okada, K.; Kakiuchi, S.; Zembutsu, H.; Furukawa, F.; Kawamura, M.; Kobayashi, K.; Imai, K.; Nakamura, Y. *Oncogene* **2003**, *22*, 2192.
16. Gasnereau, I.; Boissan, M.; Margall-Ducos, G.; Couchy, G.; Wendum, D.; Bourgain-Guglielmetti, F.; Desdouets, C.; Lacombe, M. L.; Zucman-Rossi, J.; Sobczak-Thépot, J. *Am. J. Pathol.* **2012**, *180*, 131.
17. Yamashita, J.; Fukushima, S.; Jinnin, M.; Honda, N.; Makino, K.; Sakai, K.; Masuguchi, S.; Inoue, Y.; Ihn, H. *Acta Derm. Venereol.* **2012**, *92*, 593.
18. Claerhout, S.; Lim, J. Y.; Choi, W.; Park, Y. Y.; Kim, K.; Kim, S. B.; Lee, J. S.; Mills, G. B.; Cho, J. Y. *PLoS ONE* **2011**, *6*, e24662.
19. Lai, F.; Fernald, A. A.; Zhao, N.; Le Beau, M. M. *Gene* **2000**, *248*, 117.
20. Gruneberg, U.; Neef, R.; Honda, R.; Nigg, E. A.; Barr, F. A. *J. Cell Biol.* **2004**, *166*, 167.
21. Carmena, M.; Wheelock, M.; Funabiki, H.; Earnshaw, W. C. *Nat. Rev. Mol. Cell Biol.* **2012**, *13*, 789.
22. Verhey, K. J.; Hammond, J. W. *Nat. Rev. Mol. Cell Biol.* **2009**, *10*, 765.
23. Hirokawa, N.; Noda, Y.; Tanaka, Y.; Niwa, S. *Nat. Rev. Mol. Cell Biol.* **2009**, *10*, 682.
24. Tcherniuk, S.; Skoufias, D. A.; Labriere, C.; Rath, O.; Gueritte, F.; Guillou, C.; Kozielski, F. *Angew. Chem., Int. Ed.* **2010**, *49*, 8228.
25. Khongkow, P.; Gomes, A. R.; Gong, C.; Man, E. P.; Tsang, J. W.; Zhao, F.; Monteiro, L. J.; Coombes, R. C.; Medema, R. H.; Khoo, U. S.; Lam, E. W. *Oncogene* **2015**, *1*.
26. Guillou, C.; Kozielski, F.; Labriere, C.; Gueritte, F.; Skoufias, D. A.; Tcherniuk, S.; Thal, C.; Husson, H. P. PCT WO2010150211, 2010.
27. Compound **4d** has been previously synthesized see Kawamoto, I.; Kaneko, S.; Sakurai, M.; Muramatsu, Y.; (Sankyo Co., Ltd, Japan). Application JP 2000336075, 2000.
28. Boschi, D.; Tron, G. C.; Lazzarato, L.; Chegaev, K.; Cena, C.; Di Stilo, A.; Giorgis, M.; Bertinaria, M.; Fruttero, R.; Gasco, A. *J. Med. Chem.* **2006**, *49*, 2886.
29. For the preparation of compound **7d** see: Drost, K. J.; Jones, R. J.; Cava, M. P. *J. Org. Chem.* **1989**, *54*, 5985.
30. For the preparation of compound **7g** see: Elokda, H. M.; Sie-Yearl, C.; Sulkowski, T. S. US patent 005710164A, 1998.
31. Mistry, A. G.; Smith, K.; Bye, M. R. *Tetrahedron Lett.* **1986**, *1051*, 27.
32. Slaett, J.; Romero, I.; Bergman, J. *Synthesis* **2004**, 2760.
33. Hagedorn, I.; Hohler, W. *Angew. Chem., Int. Ed.* **1975**, *14*, 486.
34. Tcherniuk, S.; Deshayes, S.; Sarli, V.; Divita, G.; Abrieu, A. *Chem. Biol.* **2011**, *18*, 631.
35. Zavala, F.; Guenard, D.; Robin, J. P.; Brown, E. *J. Med. Chem.* **1980**, *23*, 546.
36. Latate, H.; Senilh, V.; Wright, M.; Guenard, D.; Potier, P. *Proc. Natl Acad. Sci. U.S. A.* **1984**, *81*, 4090.